



Discovery of the First Low-luminosity Quasar at $z > 7$

Yoshiki Matsuoka¹, Masafusa Onoue², Nobunari Kashikawa^{3,4,5}, Michael A Strauss⁶, Kazushi Iwasawa⁷, Chien-Hsiu Lee⁸, Masatoshi Imanishi^{4,5}, Tohru Nagao¹, Masayuki Akiyama⁹, Naoko Asami¹⁰, James Bosch⁶, Hisanori Furusawa⁴, Tomotsugu Goto¹¹, James E Gunn⁶, Yuichi Harikane^{12,13}, Hiroyuki Ikeda⁴, Takuma Izumi⁴, Toshihiro Kawaguchi¹⁴, Nanako Kato¹⁵, Satoshi Kikuta^{4,5}, Kotaro Kohno^{16,17}, Yutaka Komiyama^{4,5}, Shuhei Koyama¹, Robert H Lupton⁶, Takeo Minezaki¹⁶, Satoshi Miyazaki^{4,5}, Hitoshi Murayama¹⁸, Mana Niida¹⁵, Atsushi J Nishizawa¹⁹, Akatoki Noboriguchi¹⁵, Masamune Oguri^{13,17,18}, Yoshiaki Ono¹², Masami Ouchi^{12,18}, Paul A Price⁶, Hiroaki Sameshima²⁰, Andreas Schulze⁴, Hikari Shirakata²¹, John D Silverman¹⁸, Naoshi Sugiyama^{18,22}, Philip J Tait²³, Masahiro Takada¹⁸, Tadafumi Takata^{4,5}, Masayuki Tanaka^{4,5}, Ji-Jia Tang²⁴, Yoshiki Toba^{24,25}, Yousuke Utsumi²⁶, Shiang-Yu Wang²⁴, and Takuji Yamashita¹

¹ Research Center for Space and Cosmic Evolution, Ehime University, Matsuyama, Ehime 790-8577, Japan; yk.matsuoka@cosmos.ehime-u.ac.jp

² Max Planck Institut für Astronomie, Königstuhl 17, D-69117, Heidelberg, Germany

³ Department of Astronomy, School of Science, The University of Tokyo, Tokyo 113-0033, Japan

⁴ National Astronomical Observatory of Japan, Mitaka, Tokyo 181-8588, Japan

⁵ Department of Astronomical Science, Graduate University for Advanced Studies (SOKENDAI), Mitaka, Tokyo 181-8588, Japan

⁶ Princeton University Observatory, Peyton Hall, Princeton, NJ 08544, USA

⁷ ICREA and Institut de Ciències del Cosmos, Universitat de Barcelona, IEEC-UB, Martí i Franquès, 1, E-08028 Barcelona, Spain

⁸ National Optical Astronomy Observatory, 950 North Cherry Avenue, Tucson, AZ 85719, USA

⁹ Astronomical Institute, Tohoku University, Aoba, Sendai, 980-8578, Japan

¹⁰ Seisa University, Hakone-machi, Kanagawa, 250-0631, Japan

¹¹ Institute of Astronomy and Department of Physics, National Tsing Hua University, Hsinchu 30013, Taiwan

¹² Institute for Cosmic Ray Research, The University of Tokyo, Kashiwa, Chiba 277-8582, Japan

¹³ Department of Physics, Graduate School of Science, The University of Tokyo, Bunkyo, Tokyo 113-0033, Japan

¹⁴ Department of Economics, Management and Information Science, Onomichi City University, Onomichi, Hiroshima 722-8506, Japan

¹⁵ Graduate School of Science and Engineering, Ehime University, Matsuyama, Ehime 790-8577, Japan

¹⁶ Institute of Astronomy, The University of Tokyo, Mitaka, Tokyo 181-0015, Japan

¹⁷ Research Center for the Early Universe, University of Tokyo, Tokyo 113-0033, Japan

¹⁸ Kavli Institute for the Physics and Mathematics of the Universe, WPI, The University of Tokyo, Kashiwa, Chiba 277-8583, Japan

¹⁹ Institute for Advanced Research, Nagoya University, Furo-cho, Chikusa-ku, Nagoya 464-8602, Japan

²⁰ Koyama Astronomical Observatory, Kyoto-Sangyo University, Kita, Kyoto, 603-8555, Japan

²¹ Department of Cosmoscience, Graduate School of Science, Hokkaido University, N10 W8, Kitaku, Sapporo 060-0810, Japan

²² Graduate School of Science, Nagoya University, Furo-cho, Chikusa-ku, Nagoya 464-8602, Japan

²³ Subaru Telescope, Hilo, HI 96720, USA

²⁴ Institute of Astronomy and Astrophysics, Academia Sinica, Taipei, 10617, Taiwan

²⁵ Department of Astronomy, Kyoto University, Sakyo-ku, Kyoto, Kyoto 606-8502, Japan

²⁶ Kavli Institute for Particle Astrophysics and Cosmology, Stanford University, CA 94025, USA

Received 2019 January 15; revised 2019 January 27; accepted 2019 January 28; published 2019 February 6

Abstract


We report the discovery of a quasar at $z = 7.07$, which was selected from the deep multi-band imaging data collected by the Hyper Suprime-Cam (HSC) Subaru Strategic Program survey. This quasar, HSC J124353.93+010038.5, has an order of magnitude lower luminosity than do the other known quasars at $z > 7$. The rest-frame ultraviolet absolute magnitude is $M_{1450} = -24.13 \pm 0.08$ mag and the bolometric luminosity is $L_{\text{bol}} = (1.4 \pm 0.1) \times 10^{46}$ erg s⁻¹. Its spectrum in the optical to near-infrared shows strong emission lines, and shows evidence for a fast gas outflow, as the C IV line is blueshifted and there is indication of broad absorption lines. The Mg II-based black hole mass is $M_{\text{BH}} = (3.3 \pm 2.0) \times 10^8 M_{\odot}$, thus indicating a moderate mass accretion rate with an Eddington ratio $\lambda_{\text{Edd}} = 0.34 \pm 0.20$. It is the first $z > 7$ quasar with sub-Eddington accretion, besides being the third most distant quasar known to date. The luminosity and black hole mass are comparable to, or even lower than, those measured for the majority of low- z quasars discovered by the Sloan Digital Sky Survey, and thus this quasar likely represents a $z > 7$ counterpart to quasars commonly observed in the low- z universe.

Key words: dark ages, reionization, first stars – galaxies: active – galaxies: high-redshift – intergalactic medium – quasars: general – quasars: supermassive black holes

1. Introduction

Quasars residing in the first billion years of the universe ($z > 5.7$) have been used as various types of probes into early

cosmic history. The progress of cosmic reionization can be estimated from HI absorption imprinted on the rest-frame ultraviolet spectrum of a high- z quasar; this absorption is very sensitive to the neutral fraction of the foreground intergalactic medium (IGM; Gunn & Peterson 1965; Fan et al. 2006). The luminosity and mass functions of quasars reflect the seeding and growth mechanisms of supermassive black holes (SMBHs), which can be studied through comparison with

 Original content from this work may be used under the terms of the [Creative Commons Attribution 3.0 licence](https://creativecommons.org/licenses/by/3.0/). Any further distribution of this work must maintain attribution to the author(s) and the title of the work, journal citation and DOI.

theoretical models (e.g., Volonteri 2012; Ferrara et al. 2014; Madau et al. 2014). Measurements of quasar host galaxies and surrounding environments tell us about the earliest mass assembly, possibly happening in the highest-density peaks of the underlying dark matter distribution (e.g., Goto et al. 2009; Decarli et al. 2017; Izumi et al. 2018).

Quasars at the highest redshifts are of particular interest, as they exist in the shortest period of time after the Big Bang. The current frontier for high- z quasar searches is $z > 7$, where only a few quasars have been found to date. Because radiation from $z > 7$ quasars is almost completely absorbed by the IGM at observed wavelengths $\lambda < 9700 \text{ \AA}$ and such objects are very rare and faint, one needs wide-field deep imaging in near-infrared (IR) bands or in the y -band with red-sensitive charge-coupled devices (CCDs) to discover those quasars. The first $z > 7$ quasar was discovered by Mortlock et al. (2011) at $z = 7.09$, from the United Kingdom Infrared Telescope Infrared Deep Sky Survey (UKIDSS; Lawrence et al. 2007) data. The second one was discovered by Bañados et al. (2018) at $z = 7.54$, by combining data from the *Wide-field Infrared Survey Explorer* (Wright et al. 2010), UKIDSS, and the Dark Energy Camera Legacy Survey.²⁷ In addition, two quasars, both at $z = 7.02$, were recently discovered (Wang et al. 2018; Yang et al. 2018) by combining data sets from several wide-field surveys, including the Dark Energy Survey (The Dark Energy Survey Collaboration 2005), the Dark Energy Spectroscopic Instrument legacy imaging surveys (Dey et al. 2018), and the Panoramic Survey Telescope & Rapid Response System 1 (Pan-STARRS1; Chambers et al. 2016).

However, the above $z > 7$ quasars are all very luminous (if they are not strongly lensed; e.g., Fan et al. 2019; Pacucci & Loeb 2019), due to the detection limits of the imaging survey observations. These quasars harbor SMBHs with masses of roughly a billion solar masses, shining at close to the Eddington luminosity (however, the black hole mass of one of the quasars at $z = 7.02$ has not been measured; Yang et al. 2018). They likely represent the most extreme monsters, which are very rare at all redshifts, especially at $z > 7$. To understand a wider picture of the formation and early evolution of SMBHs, it is crucial to find $z > 7$ quasars of more typical luminosity, which would be direct counterparts to low- z ordinary quasars.

This Letter presents the discovery of a quasar at $z = 7.07$, HSC J124353.93+010038.5 (hereafter “J1243+0100”), which has an order of magnitude lower luminosity than do the other known $z > 7$ quasars. It harbors an SMBH with a mass of $M_{\text{BH}} = (3.3 \pm 2.0) \times 10^8 M_{\odot}$ and shining at an Eddington ratio $\lambda_{\text{Edd}} = 0.34 \pm 0.20$. We describe the target selection and spectroscopic observations in Section 2. The spectral properties of the quasar are measured and discussed in Section 3. A summary appears in Section 4. We adopt the cosmological parameters $H_0 = 70 \text{ km s}^{-1} \text{ Mpc}^{-1}$, $\Omega_{\text{M}} = 0.3$, and $\Omega_{\Lambda} = 0.7$. All magnitudes refer to point-spread function (PSF) magnitudes in the AB system (Oke & Gunn 1983), and are corrected for Galactic extinction (Schlegel et al. 1998).

2. Observations

J1243+0100 was selected from the Hyper Suprime-Cam (HSC) Subaru Strategic Program (SSP) survey (Aihara et al. 2018a) data, as a part of the Subaru High- z Exploration of

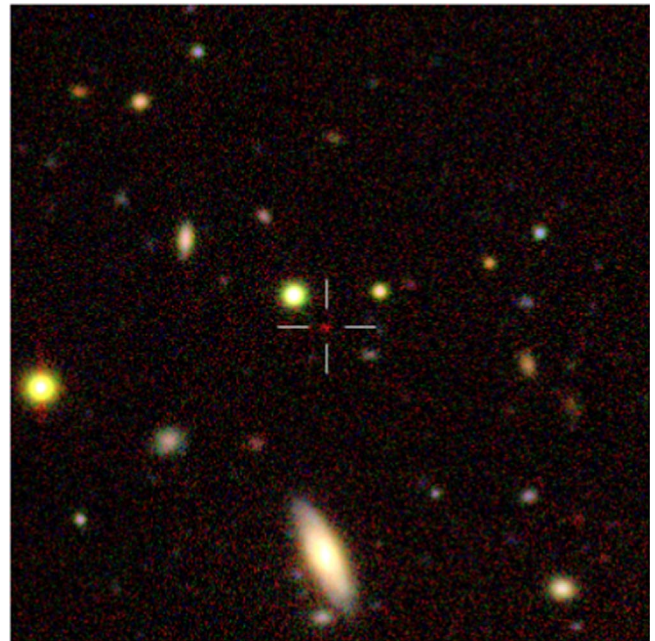


Figure 1. Three-color (HSC i -, z -, and y -band) composite image around J1243+0100, marked with the cross-hair. The image size is 1 arcmin on a side. North is up and east is to the left.

Table 1
Coordinates^a and Brightness

R.A.	12 ^h 43 ^m 53 ^s .93
Decl.	+01 ^o 00′38″.5
g_{AB} (mag)	<26.7 (2σ)
r_{AB} (mag)	<26.5 (2σ)
i_{AB} (mag)	<26.7 (2σ)
z_{AB} (mag)	<25.8 (2σ)
y_{AB} (mag)	23.57 \pm 0.08
m_{1450} (mag)	22.82 \pm 0.08
M_{1450} (mag)	−24.13 \pm 0.08
L_{bol} (erg s ^{−1})	(1.4 \pm 0.1) $\times 10^{46}$

Note.

^a Coordinates are at J2000.0. The astrometric accuracy of the HSC-SSP data is estimated to be 0″.1 (Aihara et al. 2018b).

Low-Luminosity Quasars (SHELLQs) project (Matsuoka et al. 2016, 2018a, 2018b, 2018c). The coordinates and brightness are summarized in Table 1. A three-color composite image around the quasar is presented in Figure 1. This source has an FWHM size of 0″.7 on the y -band image, which is consistent with the PSF size estimated at the corresponding image position. We used the methods detailed in Matsuoka et al. (2018b) to select this source as a high- z quasar candidate. The probability that this source was a quasar, not a Galactic brown dwarf, was $P_{\text{Q}} = 0.4$, based on our Bayesian probabilistic algorithm (Matsuoka et al. 2016) and the HSC i -, z -, and y -band photometry. It is among ~ 30 z -band dropout objects in our quasar candidate list; we have so far conducted follow-up observations of roughly half of these candidates, and partly reported the results in the SHELLQs papers mentioned above. The highest- z quasar we found and published previously is at $z \sim 6.9$ (Matsuoka et al. 2018a).

We obtained a red-optical spectrum of the candidate using the Faint Object Camera and Spectrograph (FOCAS; Kashikawa et al. 2002) mounted on the Subaru telescope. The observations were carried out on 2018 April 24 as a part of a Subaru intensive

²⁷ <http://legacysurvey.org/decamls>

program (program ID: S16B-011I). We used FOCAS in the multi-object spectrograph mode with the VPH900 grism and SO58 order-sorting filter. With a slit width of $1''.0$, this configuration gave spectral coverage from 0.75 to $1.05 \mu\text{m}$ and resolution $R \sim 1200$. We took 7×10 minutes exposures with $1''$ dithering between exposures along the slit, under photometric skies with the seeing around $0''.6$. The data were reduced with IRAF using the dedicated FOCASRED package in the standard manner. The wavelength scale was calibrated with reference to sky emission lines, and the flux calibration was tied to a white dwarf standard star, Feige 34, observed on the same night. The slit loss was corrected for by scaling the spectrum to match the HSC y -band magnitude (Table 1).

A near-IR spectrum of the object was obtained with the Gemini Near-InfraRed Spectrograph (GNIRS; Elias et al. 2006) on the Gemini-north telescope. The observations were carried out on 2018 June 25, July 22, and July 29 in the queue mode (program ID: GN-2018A-FT-112). We used the cross-dispersed mode with $321/\text{mm}$ grating, with the central wavelength set to $1.65 \mu\text{m}$. The slit width was $1''.0$, which gave spectral coverage from 0.85 to $2.5 \mu\text{m}$ and resolution $R \sim 500$. We took 36×5 minutes exposures in total, with $3''$ dithering between exposures along the slit, under spectroscopic skies with the seeing $0''.5$ – $0''.7$. The data reduction was performed with IRAF using the Gemini GNIRS package, in the standard manner. The wavelength scale was calibrated with reference to Argon lamp spectra, and the flux calibration and telluric absorption correction were tied to a standard star, HIP 58510, observed right before or after the quasar observations at similar airmass. We scaled the GNIRS spectrum to match the FOCAS spectrum in the overlapping wavelength range.

In addition, we took a K -band spectrum of the quasar with the Multi-Object Infrared Camera and Spectrograph (MOIRCS; Ichikawa et al. 2006) on the Subaru telescope. The observations were carried out on 2018 July 8 and 9 (program ID: S18A-061). We used MOIRCS in the multi-object spectrograph mode with the VPH- K grism. The slit width was $0''.8$, which gave spectral coverage from 1.8 to $2.5 \mu\text{m}$ and resolution $R \sim 1700$. We took 34×4 minutes exposures in total, with $3''$ dithering between exposures along the slit, under spectroscopic skies with the seeing $0''.5$ – $0''.8$. The data reduction was performed with IRAF using the MCSMDP package, in the standard manner. The wavelength scale was calibrated with reference to sky emission lines, and the flux calibration and telluric absorption correction were tied to a standard star, HIP 69747, observed right after the quasar observations. We scaled the MOIRCS spectrum to match the GNIRS spectrum in the overlapping wavelength range.

Finally, the FOCAS, GNIRS, and MOIRCS data were merged into a single spectrum, with a wavelength pixel spacing of $\lambda/\Delta\lambda = 1500$. The associated errors were derived from the sky background spectrum measured for each of the above observations, and were propagated to the final spectrum. Figure 2 presents the merged spectrum and errors, which are used for the measurements described in the following section. While the spectrum may show marginally positive flux in the Gunn & Peterson (1965) trough bluewards of $\text{Ly}\alpha$, these are likely due to imperfect sky subtraction, as we see no signal at $<0.98 \mu\text{m}$ in the 2d spectrum. The Mg II line appears to have two peaks, but these peaks do not appear consistently among the individual exposures and are likely due to noise.

3. Spectral Measurements

We measured spectral properties of the quasar through model fitting. The model consists of a power-law continuum with a slope $\alpha_\lambda = -1.5$ (Vanden Berk et al. 2001),²⁸ Balmer continuum (De Rosa et al. 2011), Fe II + Fe III pseudo-continuum (Vestergaard & Wilkes 2001; Tsuzuki et al. 2006, modified following Kurk et al. 2007), and Gaussian profiles to represent the C IV $\lambda 1549$, C III] $\lambda 1909$, and Mg II $\lambda 2800$ emission lines. Each emission line was modeled with a single Gaussian, given the limited signal-to-noise ratio (S/N) of the spectrum. The fitting was performed in the rest-frame wavelength range from $\lambda_{\text{rest}} = 1450$ to 3000 \AA , which contains the three emission lines listed above.²⁹ All model components were fitted simultaneously to the data via χ^2 minimization, which provided the best-fit parameter values and associated errors. The derived best-fit model is presented in Figure 2.

We measured the apparent and absolute magnitudes of the quasar at $\lambda_{\text{rest}} = 1450 \text{ \AA}$ from the best-fit power-law continuum. We also measured the continuum luminosity at $\lambda_{\text{rest}} = 3000 \text{ \AA}$ from the best-fit model, and converted to the bolometric luminosity assuming a bolometric correction factor $\text{BC}_{3000} = 5.15$ (Shen et al. 2011). The results are listed in Table 1.

Table 2 summarizes the emission line properties derived from the best-fit Gaussian models. The quasar redshift measured from the Mg II line is $z = 7.07 \pm 0.01$. We found that the emission lines from the higher ionization species, C IV in particular, are significantly blueshifted relative to Mg II. We estimated the black hole mass (M_{BH}) from the FWHM of Mg II and the continuum luminosity at $\lambda_{\text{rest}} = 1350 \text{ \AA}$, using the calibration presented by Vestergaard & Osmer (2009).³⁰ This yielded $M_{\text{BH}} = (3.3 \pm 2.0) \times 10^8 M_\odot$, and an Eddington ratio $\lambda_{\text{Edd}} = 0.34 \pm 0.20$. The systematic uncertainty of the above calibration is estimated to be a factor of a few, which is not included in the M_{BH} and λ_{Edd} errors presented in this Letter.

The $\text{Ly}\alpha$ strength relative to the above emission lines appears weaker than observed in low- z quasars (e.g., Vanden Berk et al. 2001). This is likely due to IGM absorption, including damping wing absorption redwards of $\text{Ly}\alpha$, and/or possible BALs. We defer detailed modeling of these absorptions to a future paper, and here measured the $\text{Ly}\alpha + \text{NV } \lambda 1240$ flux by simply integrating observed flux excess above the continuum model over $\lambda_{\text{rest}} = 1215$ – 1255 \AA ; the result is listed in Table 2.

Figure 3 compares the estimated black hole mass and bolometric luminosity of J1243+0100 with those of other quasars in the literature. While the other known $z > 7$ quasars have $M_{\text{BH}} \gtrsim 10^9 M_\odot$ and radiate at the rates close to the Eddington limit, J1243+0100 has a considerably lower-mass black hole and is shining at a sub-Eddington rate. The

²⁸ We also tried fitting with a variable slope and found that this parameter is poorly constrained ($\alpha_\lambda = -2.0 \pm 0.8$), presumably due to degeneracy with the other continuum components and the limited S/N of the present data.

²⁹ We did not include in the fitting the spectral region around Si IV $\lambda 1400$, which is affected by the low atmospheric transmission and possibly by broad absorption lines (BALs; see below).

³⁰ We could use the continuum luminosity estimated at a wavelength closer to the Mg II line, but given the limited S/N of the present data, the measurement would be affected by the degeneracy of the three (power-law, Balmer, and iron) continuum components. We checked that the M_{BH} estimate does not change significantly when the continuum luminosity at 2100 or 3000 \AA is used alternatively, with the corresponding calibration factor from Vestergaard & Osmer (2009).

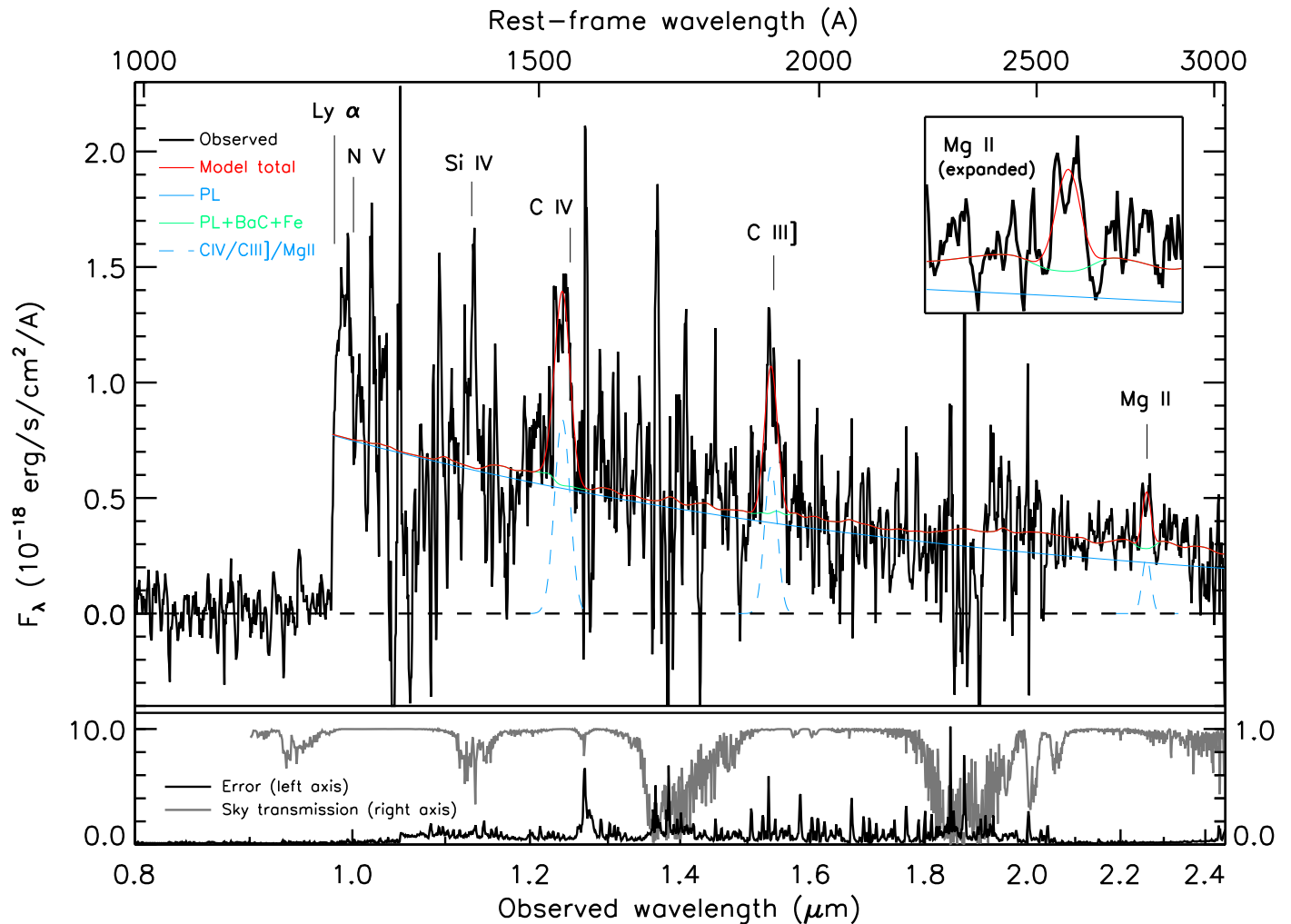


Figure 2. Upper panel: the merged FOCAS, GNIRS, and MOIRCS spectrum of J1243+0100, smoothed using inverse-variance weighted means in 5 pixel for display purpose (black line). The expected positions of strong emission lines are marked by the vertical lines, given the Mg II-based redshift. Also plotted is the best-fit model spectrum (red line), which is the sum of a power-law continuum (blue solid line), Balmer and iron continua (the green solid line represents the sum of these two components plus the power-law continuum), the emission lines of C IV $\lambda 1549$, C III] $\lambda 1909$, and Mg II $\lambda 2800$ (blue dashed lines). The dips of observed flux relative to the power-law continuum model at $\sim 1.05 \mu\text{m}$ and $\sim 1.17 \mu\text{m}$ may be due to broad absorption lines. The insert shows an expanded view of the spectrum around Mg II. Lower panel: the error spectrum (black line) and the atmospheric transmission spectrum above Maunakea (Lord 1992, data retrieved from Gemini Observatory and plotted in gray).

luminosity and black hole mass of J1243+0100 are comparable to, or even lower than, those measured for the majority of low- z quasars in the Sloan Digital Sky Survey (SDSS) Data Release 7 (DR7) catalog (Shen et al. 2011). Thus, this quasar likely represents the first example of an ordinary quasar beyond $z = 7$.

On the other hand, given the limited S/N of the spectrum, the present measurements of M_{BH} and λ_{Edd} could be biased; for example, noise spikes can affect measurement of the Mg II line width significantly. We added artificial errors to the spectrum, based on the observed noise array, and performed the model fitting for 100 realizations of the generated spectrum. This yielded $M_{\text{BH}} = (3.1 \pm 1.3) \times 10^8 M_{\odot}$ and $\lambda_{\text{Edd}} = 0.36 \pm 0.16$ (the median values and intervals containing 68% of the realizations), while 5% and 2% of the realizations gave ($M_{\text{BH}} < 10^8 M_{\odot}$, $\lambda_{\text{Edd}} \geq 1$) and ($M_{\text{BH}} > 10^9 M_{\odot}$, $\lambda_{\text{Edd}} < 0.1$), respectively. Deeper observations than those presented here are clearly needed to better characterize this quasar.

J1243+0100 has strong emission lines with high equivalent widths, compared to the luminous $z > 7$ quasars, which may in part reflect the so-called Baldwin (1977) effect. We found that

the rest-frame equivalent widths (REWs) of the emission lines listed in Table 2 are comparable to those of low- z counterparts. In particular, the median REWs of $\sim 13,000$ SDSS DR7 quasars, selected to have continuum luminosities within ± 0.1 dex of J1243+0100, are 49 \AA and 36 \AA for C IV and Mg II, respectively. This may indicate that the physical conditions in the broad line regions of quasars are similar from $z > 7$ to the relatively nearby universe. In addition, the spectrum of J1243+0100 may show signs of BALs blueward of the Si IV and C IV emission lines. While these features are found at wavelengths relatively free from atmospheric absorption, the limited S/N of the present data prevents us from robustly confirming them. This possible BAL signature and the large blueshift of the C IV emission line may indicate the presence of a fast gas outflow close to the quasar nucleus.

An important application of a high- z quasar spectrum is to measure the IGM neutral fraction around the quasar via the absorption damping wing analysis. One could also estimate the quasar lifetime from an analysis of the quasar near-zone size. However, such measurements require accurate modeling of the

Table 2
Emission Line Measurements

	Ly α + N V λ 1240	C IV λ 1549	C III] λ 1909	Mg II λ 2800
Redshift	7.07 ± 0.01
Velocity Offset (km s $^{-1}$)	...	-2400 ± 500	-800 ± 400	...
Flux (erg s $^{-1}$ cm $^{-2}$)	$(9.6 \pm 0.4) \times 10^{-17}$	$(2.1 \pm 0.4) \times 10^{-16}$	$(1.6 \pm 0.5) \times 10^{-16}$	$(6.2 \pm 1.9) \times 10^{-17}$
Rest-frame Equivalent Widths (\AA)	16 ± 1	48 ± 10	51 ± 15	35 ± 11
FWHM (km s $^{-1}$)	...	5500 ± 1300	4600 ± 1500	3100 ± 900
M_{BH} (M_{\odot})	$(3.3 \pm 2.0) \times 10^8$
λ_{Edd}	0.34 ± 0.20

Note. The velocity offsets were measured relative to Mg II λ 2800. The FWHMs were corrected for the instrumental velocity resolution.

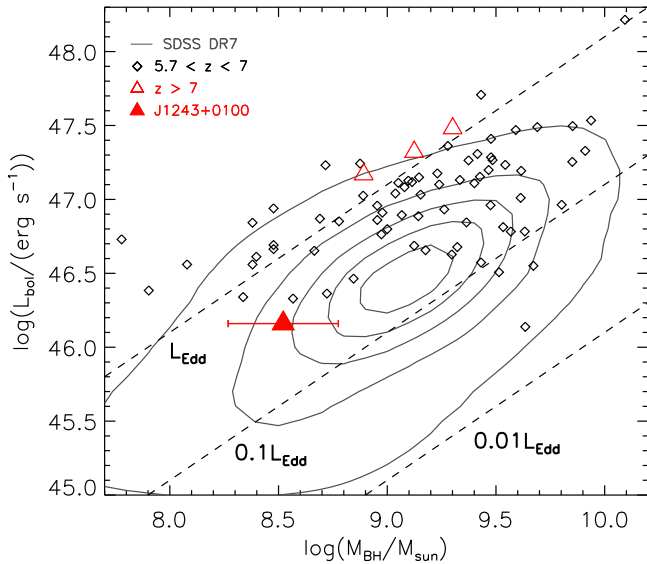


Figure 3. Compilation of black hole mass and bolometric luminosity measurements in quasars. The contours (linearly spaced in surface density) represent the distribution of quasars in the SDSS DR7 catalog (Shen et al. 2011), while the diamonds represent quasars at $5.7 < z < 7$ (Jiang et al. 2007; Kurk et al. 2007; Willott et al. 2010; De Rosa et al. 2011, 2014; Venemans et al. 2015; Wu et al. 2015; Mazzucchelli et al. 2017; Eilers et al. 2018; Shen et al. 2018). The filled triangle represents J1243+0100, the quasar presented in this Letter, while the unfilled triangles represent other $z > 7$ quasars reported by Mortlock et al. (2011), Bañados et al. (2018), and Wang et al. (2018).

spectral shape around Ly α , which is hard to do with the limited S/N of the present data. The BAL features, if confirmed to be present, may also complicate such analyses for J1243+0100. But these will be interesting subjects of follow-up studies, with deeper spectroscopy in the optical and near-IR. Finally, future observations of this highest- z ordinary quasar with, e.g., the Atacama Large Millimeter/submillimeter Array and the *James Webb Space Telescope*, will allow us to investigate the gaseous and stellar properties of the host galaxy, and will be key to understanding the relationship between the quasar activity and the host galaxy at an early stage of cosmic history.

4. Summary

This Letter is the seventh in a series of publications presenting the results from the SHELLQs project, a search for low-luminosity quasars at $z \gtrsim 6$ based on the deep multi-band imaging data produced by the HSC-SSP survey. We presented the discovery of J1243+0100, a quasar at $z = 7.07$. It was selected as a quasar candidate from the HSC data, and its optical to near-IR spectrum was obtained with FOCAS and MOIRCS on Subaru, and GNIRS on Gemini. The quasar has

an order of magnitude lower luminosity than other known quasars at $z > 7$. The estimated black hole mass is $M_{\text{BH}} = (3.3 \pm 2.0) \times 10^8 M_{\odot}$, and the Eddington ratio is $\lambda_{\text{Edd}} = 0.34 \pm 0.20$. As such, this quasar may represent the first example of an ordinary quasar beyond $z = 7$. The large blueshift of the C IV emission line and possible BAL features suggest the presence of a fast gas outflow close to the quasar nucleus.

The discovery of J1243+0100 demonstrates the power of the HSC-SSP survey to explore SMBHs at $z > 7$, with masses typical of lower- z quasars. The quasar was selected from $\sim 900 \text{ deg}^2$ of the survey (including substantial area with partial survey depths), and we are in the course of follow-up observations of the remaining candidates. We expect to find a few more quasars at $z > 7$ by the completion of the survey, which is going to cover 1400 deg^2 in the wide layer. Combined with luminous $z > 7$ quasars discovered by other surveys, and also with lower- z counterparts of ordinary quasars, those high- z low-luminosity quasars will provide a significant insight into the formation and evolution of SMBHs across cosmic history.

This work is based on data collected at the Subaru Telescope and retrieved from the HSC data archive system, which is operated by the Subaru Telescope and Astronomy Data Center at National Astronomical Observatory of Japan (NAOJ). The data analysis was in part carried out on the open use data analysis computer system at the Astronomy Data Center of NAOJ.

This work is also based on observations obtained at the Gemini Observatory and processed using the Gemini IRAF package. The Observatory is operated by the Association of Universities for Research in Astronomy, Inc., under a cooperative agreement with the NSF on behalf of the Gemini partnership: the National Science Foundation (United States), the National Research Council (Canada), CONICYT (Chile), Ministerio de Ciencia, Tecnología e Innovación Productiva (Argentina), and Ministério da Ciência, Tecnologia e Inovação (Brazil).

Y.M. was supported by the Japan Society for the Promotion of Science (JSPS) KAKENHI grant No. JP17H04830 and the Mitsubishi Foundation grant No. 30140. N.K. acknowledges supports from the JSPS grant 15H03645. K.I. acknowledges support by the Spanish MINECO under grant No. AYA2016-76012-C3-1-P and MDM-2014-0369 of ICCUB (Unidad de Excelencia “María de Maeztu”).

The Hyper Suprime-Cam (HSC) collaboration includes the astronomical communities of Japan and Taiwan, and Princeton University. The HSC instrumentation and software were developed by the National Astronomical Observatory of Japan (NAOJ), the Kavli Institute for the Physics and Mathematics of the Universe (Kavli IPMU), the University of Tokyo, the High






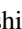











Energy Accelerator Research Organization (KEK), the Academia Sinica Institute for Astronomy and Astrophysics in Taiwan (ASIAA), and Princeton University. Funding was contributed by the FIRST program from Japanese Cabinet Office, the Ministry of Education, Culture, Sports, Science and Technology (MEXT), the Japan Society for the Promotion of Science (JSPS), Japan Science and Technology Agency (JST), the Toray Science Foundation, NAOJ, Kavli IPMU, KEK, ASIAA, and Princeton University.










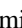


The Pan-STARRS1 Surveys (PS1) have been made possible through contributions of the Institute for Astronomy, the University of Hawaii, the Pan-STARRS Project Office, the Max-Planck Society and its participating institutes, the Max Planck Institute for Astronomy, Heidelberg and the Max Planck Institute for Extraterrestrial Physics, Garching, The Johns Hopkins University, Durham University, the University of Edinburgh, Queen's University Belfast, the Harvard-Smithsonian Center for Astrophysics, the Las Cumbres Observatory Global Telescope Network Incorporated, the National Central University of Taiwan, the Space Telescope Science Institute, the National Aeronautics and Space Administration under grant No. NNX08AR22G issued through the Planetary Science Division of the NASA Science Mission Directorate, the National Science Foundation under grant No. AST-1238877, the University of Maryland, and Eotvos Lorand University (ELTE).

This Letter makes use of software developed for the Large Synoptic Survey Telescope. We thank the LSST Project for making their code available as free software at <http://dm.lsst.org>.

IRAF is distributed by the National Optical Astronomy Observatory, which is operated by the Association of Universities for Research in Astronomy (AURA) under a cooperative agreement with the National Science Foundation.

ORCID iDs

Masafusa Onoue  <https://orcid.org/0000-0003-2984-6803>
 Nobunari Kashikawa  <https://orcid.org/0000-0001-5493-6259>
 Michael A Strauss  <https://orcid.org/0000-0002-0106-7755>
 Kazushi Iwasawa  <https://orcid.org/0000-0002-4923-3281>
 Chien-Hsiu Lee  <https://orcid.org/0000-0003-1700-5740>
 Masatoshi Imanishi  <https://orcid.org/0000-0001-6186-8792>
 Tohru Nagao  <https://orcid.org/0000-0002-7402-5441>
 Masayuki Akiyama  <https://orcid.org/0000-0002-2651-1701>
 James Bosch  <https://orcid.org/0000-0003-2759-5764>
 Yuichi Harikane  <https://orcid.org/0000-0002-6047-430X>
 Hiroyuki Ikeda  <https://orcid.org/0000-0002-1207-1979>
 Takuma Izumi  <https://orcid.org/0000-0001-9452-0813>
 Satoshi Kikuta  <https://orcid.org/0000-0003-3214-9128>
 Kotaro Kohno  <https://orcid.org/0000-0002-4052-2394>
 Robert H Lupton  <https://orcid.org/0000-0003-1666-0962>
 Takeo Minezaki  <https://orcid.org/0000-0002-2933-048X>
 Satoshi Miyazaki  <https://orcid.org/0000-0002-1962-904X>
 Hitoshi Murayama  <https://orcid.org/0000-0001-5769-9471>

Akatoki Noboriguchi  <https://orcid.org/0000-0002-5197-8944>
 Masamune Oguri  <https://orcid.org/0000-0003-3484-399X>
 Masami Ouchi  <https://orcid.org/0000-0002-1049-6658>
 Hiroaki Sameshima  <https://orcid.org/0000-0001-6401-723X>
 Andreas Schulze  <https://orcid.org/0000-0002-6660-6131>
 John D Silverman  <https://orcid.org/0000-0002-0000-6977>
 Masahiro Takada  <https://orcid.org/0000-0002-5578-6472>
 Tadafumi Takata  <https://orcid.org/0000-0002-6592-4250>
 Masayuki Tanaka  <https://orcid.org/0000-0002-5011-5178>
 Yoshiki Toba  <https://orcid.org/0000-0002-3531-7863>
 Yousuke Utsumi  <https://orcid.org/0000-0001-6161-8988>
 Takuji Yamashita  <https://orcid.org/0000-0002-4999-9965>

References

- Aihara, H., Arimoto, N., Armstrong, R., et al. 2018a, *PASJ*, 70, S4
 Aihara, H., Armstrong, R., Bickerton, S., et al. 2018b, *PASJ*, 70, S8
 Baldwin, J. A. 1977, *ApJ*, 214, 679
 Bañados, E., Venemans, B. P., Mazzucchelli, C., et al. 2018, *Natur*, 553, 473
 Chambers, K. C., Magnier, E. A., Metcalfe, N., et al. 2016, arXiv:1612.05560
 Decarli, R., Walter, F., Venemans, B. P., et al. 2017, *Natur*, 545, 457
 De Rosa, G., Decarli, R., Walter, F., et al. 2011, *ApJ*, 739, 56
 De Rosa, G., Venemans, B. P., Decarli, R., et al. 2014, *ApJ*, 790, 145
 Dey, A., Schlegel, D. J., Lang, D., et al. 2018, arXiv:1804.08657
 Eilers, A.-C., Hennawi, J. F., & Davies, F. B. 2018, *ApJ*, 867, 30
 Elias, J. H., Joyce, R. R., Liang, M., et al. 2006, *Proc. SPIE*, 6269, 62694C
 Fan, X., Carilli, C. L., & Keating, B. 2006, *ARA&A*, 44, 415
 Fan, X., Wang, F., Yang, J., et al. 2019, *ApJL*, 870, L11
 Ferrara, A., Salvadori, S., Yue, B., & Schleicher, D. 2014, *MNRAS*, 443, 2410
 Goto, T., Utsumi, Y., Furusawa, H., Miyazaki, S., & Komiyama, Y. 2009, *MNRAS*, 400, 843
 Gunn, J. E., & Peterson, B. A. 1965, *ApJ*, 142, 1633
 Ichikawa, T., Suzuki, R., Tokoku, C., et al. 2006, *Proc. SPIE*, 6269, 626916
 Izumi, T., Onoue, M., Shirakata, H., et al. 2018, *PASJ*, 70, 36
 Jiang, L., Fan, X., Vestergaard, M., et al. 2007, *AJ*, 134, 1150
 Kashikawa, N., Aoki, K., Asai, R., et al. 2002, *PASJ*, 54, 819
 Kurk, J. D., Walter, F., Fan, X., et al. 2007, *ApJ*, 669, 32
 Lawrence, A., Warren, S. J., Almaini, O., et al. 2007, *MNRAS*, 379, 1599
 Lord, S. D. 1992, NASA Tech. Memor 103957
 Madau, P., Haardt, F., & Dotti, M. 2014, *ApJL*, 784, L38
 Matsuoka, Y., Iwasawa, K., Onoue, M., et al. 2018a, *ApJS*, 237, 5
 Matsuoka, Y., Onoue, M., Kashikawa, N., et al. 2016, *ApJ*, 828, 26
 Matsuoka, Y., Onoue, M., Kashikawa, N., et al. 2018b, *PASJ*, 70, S35
 Matsuoka, Y., Strauss, M. A., Kashikawa, N., et al. 2018c, *ApJ*, 869, 150
 Mazzucchelli, C., Bañados, E., Venemans, B. P., et al. 2017, *ApJ*, 849, 91
 Mortlock, D. J., Warren, S. J., Venemans, B. P., et al. 2011, *Natur*, 474, 616
 Oke, J. B., & Gunn, J. E. 1983, *ApJ*, 266, 713
 Pacucci, F., & Loeb, A. 2019, *ApJL*, 870, L12
 Schlegel, D. J., Finkbeiner, D. P., & Davis, M. 1998, *ApJ*, 500, 525
 Shen, Y., Richards, G. T., Strauss, M. A., et al. 2011, *ApJS*, 194, 45
 Shen, Y., Wu, J., Jiang, L., et al. 2018, arXiv:1809.05584
 The Dark Energy Survey Collaboration, 2005, arXiv:astro-ph/0510346
 Tsuzuki, Y., Kawara, K., Yoshii, Y., et al. 2006, *ApJ*, 650, 57
 Vanden Berk, D. E., Richards, G. T., Bauer, A., et al. 2001, *AJ*, 122, 549
 Venemans, B. P., Bañados, E., Decarli, R., et al. 2015, *ApJL*, 801, L11
 Vestergaard, M., & Osmer, P. S. 2009, *ApJ*, 699, 800
 Vestergaard, M., & Wilkes, B. J. 2001, *ApJS*, 134, 1
 Volonteri, M. 2012, *Sci*, 337, 544
 Wang, F., Yang, J., Fan, X., et al. 2018, *ApJL*, 869, L9
 Willott, C. J., Albert, L., Arzoumanian, D., et al. 2010, *AJ*, 140, 546
 Wright, E. L., Eisenhardt, P. R. M., Mainzer, A. K., et al. 2010, *AJ*, 140, 1868
 Wu, X.-B., Wang, F., Fan, X., et al. 2015, *Natur*, 518, 512
 Yang, J., Wang, F., Fan, X., et al. 2018, arXiv:1811.11915